





Editorial

Editorial for Special Issue “Minerals Down to the Nanoscale: A Glimpse at Ore-Forming Processes”

Cristiana L. Ciobanu ^{1,*}, Satoshi Utsunomiya ², Martin Reich ^{3,4}, Oliver Plümper ⁵ and Nigel J. Cook ¹

¹ School of Chemical Engineering and Advanced Materials, The University of Adelaide, Adelaide, SA 5005, Australia; nigel.cook@adelaide.edu.au

² Department of Chemistry, Kyushu University, 744 Motooka, Nishi-Ku, Fukuoka-Shi 819-0395, Japan; utsunomiya.satoshi.998@m.kyushu-u.ac.jp

³ Department of Geology and Andean Geothermal Center of Excellence (CEGA), FCFM, University of Chile, Plaza Ercilla 803, Santiago 8370450, Chile; mreich@cec.uchile.cl

⁴ Millennium Nucleus for Metal Tracing Along Subduction, FCFM, University of Chile, Santiago 8370450, Chile

⁵ Department of Earth Sciences, Utrecht University, Princetonlaan 8A, 3584 CB Utrecht, The Netherlands; o.plumper@uu.nl

* Correspondence: cristiana.ciobanu@adelaide.edu.au; Tel.: +61-432-955-000

Received: 1 November 2019; Accepted: 7 November 2019; Published: 9 November 2019



1. Introduction

Minerals form in all types of chemical and physical environments. They often record superimposed geochemical processes as they react with fluids of various origins or undergo tectonothermal events when in terranes with protracted geological histories. Understanding their evolution in the context of mineral associations can provide evidence of how ore deposits formed—or, indeed, failed to form. Such glimpses of the ore-forming process can be recorded by the incorporation and release of trace elements from host minerals, the degree of order/disorder in mixed-layer compounds or complex sulphides, or the distribution of nanometer-scale inclusions relative to nanopores or reaction boundaries. Understanding such aspects is of paramount importance in tracking the robustness of mineral geochronometers, equilibrium vs. disequilibrium processes, and mass-transport and mineral reactions in confined spaces.

Nanominerals and mineral nanoparticles may behave very differently to their larger relatives—a function partly explained by differences in their surface and near-surface atomic structure, crystal shape, and surface topography [1]. These differences extend to reaction kinetics, making them of much interest across the Earth sciences and beyond. Nanoscale inclusions in ore minerals can underpin mineral formation and overprinting or provide insights into magmatic cooling paths and the magmatic-to-hydrothermal transition for common ore minerals, such as iron-oxides and sulphides, including whether these are inherited from pre-existing protoliths or form from hydrothermal fluids throughout an ore deposit lifespan. Many new insights have been obtained owing to the expanding development of analytical capability at the nanoscale, including advanced transmission electron microscopy [2], nanoSIMS, microbeam X-ray absorption spectrometry [3], and atom probe tomography [4].

In Earth sciences, the need to verify or explain observations made at the micron-scale stems from the ever expanding fields of research dealing with trace element distributions in minerals [5], phase transformation and post-crystallization/re-equilibration of minerals used as geothermobarometers [6,7], and geochronology [8]. In mineralogy, chemical-structural modularity across series of mixed-layer compounds or complexes and structures of sulfosalt homologous series can be directly assessed

using high-angle annular dark field scanning transmission electron microscopy (HAADF STEM) techniques [9–11], or conventional high-resolution transmission electron microscopy (e.g., [12]). Such minerals are prototypes for ‘smart materials’ to be used in future technological applications [13].

The unparalleled array of microanalytical instrumentation available to the contemporary researcher, including direct observation down to the scale of single atoms, can help validate or refute models and assess the evolution of complex ore-forming systems. Nanoscale observation is especially useful when combined with other complementary methods that can allow a bridging of the scales of observation from nanometers to tens of micrometers. In-situ slicing, 3D-tomography, or electron backscatter diffraction on focused ion beam (FIB) platforms provide unparalleled opportunities to bridge scales of observation on sites of petrogenetic interest [14–16].

As access to such instrumentation is becoming easier and as the importance—and often, the critical role—of ultrafine particles is being recognised, such techniques are finding ever broader application across Earth science and environmental disciplines. The results impact how geochronological data can be interpreted (e.g., [17,18]); offer potential new methods for mineral exploration (e.g., [19]); are pivotal for the extraordinarily rapid development of biomineralogy and functional nanomaterials (e.g., [20]); and can assist with tracking environmental hazards of various types, including ultra-trace level radionuclides (e.g., [21]), to mention only a few.

The rapid expansion of the research field is emphasized by the number of valuable papers published in the literature since work on this special issue commenced. We would single out the work of Yin et al. [22], who have demonstrated the important role of mineral nanoparticles at fluid–mineral interfaces during trace-element uptake in hydrothermal systems, which is a topic also discussed by several papers in this special issue.

2. The Special Issue

This special issue contains eleven papers presented in, or closely aligned to, Session 06b (Minerals Down to the Nanoscale: A Glimpse at Ore-Forming Processes) at the 2018 Goldschmidt Conference, 12–17 August, in Boston, USA. Nearly all apply nanoscale techniques to common minerals, notably iron-oxides, demonstrating that there are many aspects of these minerals that have remained hidden until now. Collectively, the analytical and experimental studies reported here demonstrate that physicochemical properties observable at the nanoscale represent important clues for elucidating the character and timing of geological processes, including, but not limited to, magmatic and hydrothermal ore genesis and associated alteration.

Crespo et al. [23] address the occurrence and mineralogical form of critical metals in porphyry copper–molybdenum deposits. In a case study of the Río Blanco-Los Bronces Cu–Mo deposit in central Chile, the authors report on the occurrence of critical metal (Pd, Pt, Au, Ag, and Te) inclusions in copper sulphides. They demonstrate, using field emission scanning electron microscopy (FESEM) techniques, the presence of nano- to micron-sized particles containing Pd, Au, and Ag. These inclusions are mostly tellurides, including merenskyite, palladian hessite, sylvanite, and petzite. Based on the data, it is proposed that Pd (and probably also Pt) is partitioned into copper sulphides during the high-temperature potassic alteration stage. This research may drive further research aimed at the mobility of platinum group elements during mineralization and partitioning into sulphides, but also the economic potential of critical metal recovery from porphyry Cu–Mo deposits.

Baurier-Aymat et al. [24] demonstrate how a study combining focused ion beam and high-resolution transmission electron microscopy can assist with the characterization of zoned inclusions of ruthenium- and osmium-bearing mineral phase laurite-erlichmanite in mantle-hosted chromitites from the Ojén ultramafic massif, southern Spain. The microscale zoning observed and quantified by SEM and an electron microprobe consists of Os-poor cores and Os-rich rims and persists to the nanoscale. The Os-poor cores consist of relatively homogenous pure laurite lacking crystal lattice defects, whereas the Os-rich rim consists of a homogenous laurite matrix hosting 10–20 nm-thick fringes of almost pure erlichmanite. Core-to-rim zoning is interpreted in terms of non-equilibrium

crystal growth. The origin of the observed zoning relates to the formation of chromitites in the Earth's upper mantle, followed by rapid cooling attributed to rapid exhumation of the rocks, preventing the effective dissolution of Os in laurite, even at ~1200 °C. The study highlights the importance and potential of nanoscale studies for an improved understanding of the genesis of platinum-group minerals in magmatic ore-forming systems.

Morishita et al. [25] use secondary ion mass spectrometry (SIMS) to address the relationship between the Au and As concentrations in pyrite and pyrrhotite from the high-sulfidation epithermal deposits of the Nansatsu district (Japan); in pyrite and pyrrhotite from the Kalahari Goldridge banded-iron-formation-hosted gold deposit (South Africa); and in pyrite from the South Deep and KDC West deposits, Witwatersrand Basin (South Africa). The authors demonstrate that the concentrations of Au in almost all the pyrites analysed lie on or below the solubility limit of Au in pyrite [26], suggesting that Au⁺ is the dominant form of Au in the studied pyrites. The morphology of pyrite from sedimentary deposits is suggested as an indicator of the hydrothermal influence on the deposit.

Xu et al. [27] address powellite-scheelite solid solution at the nanoscale in unusual samples from the Zhibula skarn, Gangdese Belt, Tibet (China), containing compositions spanning almost the full range between the two endmembers. Electron probe microanalysis shows that Mo-rich domains (from 20 mol.% to 80 mol.% powellite) occur within a matrix of unzoned, close-to-endmember scheelite. Electron diffractions, HAADF STEM imaging down to the nanoscale, STEM energy-dispersive spectroscopy (EDS) chemical mapping, and STEM simulations are used to show chemical oscillatory zoning with interfaces that have continuity in crystal orientation. Non-linear thermodynamics likely govern the patterning and presence of compositionally and texturally distinct domains, in agreement with a non-ideal solid solution. The sharpest compositional contrasts are also recognizable by variation in the growth direction. The observed geochemical and petrographic features in the sample are reconciled with a redox model involving the prograde deposition of a scheelite + molybdenite assemblage (reduced), followed by the interaction with low-T fluids, leading to molybdenite dissolution and the reprecipitation of Mo as powellite-rich domains (retrograde stage, oxidized). Last but not least, the observation of nanoscale inclusions of xenotime-(Y) within scheelite carries implications for the meaningful interpretation of scheelite petrogenesis based on rare earth element (REE) concentrations and fractionation patterns.

Gao et al. [28] report a nanoscale investigation of titanomagnetite from Fe–Ti–V ores of the Lanjiahuoshan deposit, Panzhihua layered intrusion, Southwest China. The research uses HAADF STEM imaging and STEM EDS spot analysis and mapping to establish the composition of exsolution phases and their mutual relationships in order to evaluate the sequence of exsolution and to assess mechanisms of ore formation during magma emplacement. The nanoscale evidence allows a reconstruction of the cooling history of titanomagnetite ore in terms of three distinct stages: (1) equilibrium crystallization of Al-rich, Mg-bearing titanomagnetite from cumulus melts at ~55 km, with initial exsolutions occurring above 800 °C at moderate fO_2 ; (2) crosscutting {111} exsolutions resulting in the formation of qandilite, attributable to a temperature increase due to the emplacement of additional melt affecting the interstitial cumulus during uplift; and (3) ilmenite formation from pre-existing Ti-rich spinel and ulvöspinel, illustrative of redox-driven cooling paths at <10 km.

In the first of five papers reporting nanoscale research on Cu–U–Au–Ag ores and related rocks from the Olympic Dam district, South Australia, Keyser et al. [29] document the zirconium mineralogy in a relatively coarse massive magnetite ore with a prolonged geological history. A combination of detailed petrography, electron probe microanalysis and laser ablation inductively coupled-plasma mass spectrometry (LA-ICP-MS), HAADF STEM imaging, and U–Pb zircon geochronology is used. The application of complimentary microanalytical techniques, in-situ and on the same material but at different scales, provides critical constraints on ore-forming processes and allows a reconstruction of the geological evolution of the deposit. In this model, martitization during a diagenesis and supergene enrichment cycle is followed by high-grade metamorphism, during which martite recrystallized as

granoblastic hematite. Later interaction with hydrothermal fluids associated with ~1.6 Ga granitoid rocks led to W, Sn, and Sb enrichment in the hematite.

Ciobanu et al. [30] address the question “what is silician magnetite?”, describing the results of a comprehensive nanoscale study on magnetite in samples from the outer, weakly mineralized shell at Olympic Dam, supported by STEM simulations. Silician magnetite is shown to occur as Si-Fe-nanoprecipitates that occur together with a diverse range of nanoscale inclusions of calc-silicates, as well as U-, W-(Mo), Y-As- and As-S-nanoparticles. Silician magnetite nanoprecipitates are shown to occur either with spinel-type structures or a γ -Fe_{1.5}SiO₄ phase with a maghemite structure. The two types are distinct from each another and occur as bleb-like particles and nm-wide strips along d_{111} in magnetite, respectively. The overprinting of silician magnetite during the transition from K-feldspar to sericite is expressed as abundant lattice-scale defects associated with the transformation of nanoprecipitates with a spinel structure into maghemite via Fe-vacancy ordering. The presence of silician magnetite carries petrogenetic value for defining stages of deposit evolution at Olympic Dam, and likely for iron-oxide copper gold (IOCG) systems elsewhere.

Verdugo-Ihl et al. [31] use HAADF STEM imaging and STEM EDS mapping and spot analysis on foils prepared in-situ by focused ion beam methods to characterize atypical Cu-As-zoned and weave-twinned hematite from Olympic Dam. The study reveals Cu- and Cu-As-nanoparticles, also containing mappable K, Cl, and C. The presence of internal voids with rounded morphologies, clearly revealed by high-resolution imaging, allows the nanoparticles to be interpreted as attachments to the walls of fluid inclusions, the products of replacement processes driven by coupled dissolution and reprecipitation reactions. Linear and planar defects in hematite provide evidence of strain, induced during the percolation of fluids that changed in composition from alkali-silicic to Cl- and metal-bearing brines along channels. Fluid rates evolved from slow infiltration to erratic inflow controlled by fault-valve mechanism pumping, explaining the diverse occurrence of Cu-As nanoparticles. These fluids are typical of hydrolytic alteration and the fluid pumping mechanism feasible via fault (re)activation. The nanoscale approach provides convincing evidence that fluid–mineral interactions can be fingerprinted at the (atomic) scale at which element exchange occurs.

In a provocative contribution that challenges several traditional hypotheses, Courtney-Davies et al. [32] examine nanoscale features in one of the best studies of all minerals, zircon. Based on the characterization of zircon in granites from South Australia, they present new nano- to micron-scale evidence for pervasive chemical and crystal-structural modification associated with metasomatism that occurs shortly after magmatic crystallization and preceding the onset of metamictization. Lattice stretching and screw dislocations leading to expansion of the zircon structure are the only nanoscale structures attributable to self-induced irradiation damage. Moreover, geochemical and structural modification reflect the interaction between magmatic zircon and corrosive Fe–Cl-bearing fluids in an initial metasomatic event that follows magmatic crystallization and immediately precedes the deposition of IOCG mineralization, which markedly increases the abundance of zircons from granites hosting IOCG mineralization, including Olympic Dam. A comparison of zircon geochemistry and nanostructures in granites of different ages, within and without mineralization, points to the possibility of using zircon in mineral exploration to indicate proximity to mineralization and as a potential pathfinder to locate fertile granites associated with Cu–Au mineralization.

In the last paper demonstrating the value of nanoscale studies for understanding the Olympic Dam deposit, Rollog et al. [33] demonstrate how nanoscale secondary ion mass spectrometry (nanoSIMS) can be used to map the distribution of trace components in ore and concentrate samples. In this study, nanoSIMS is used to generate chemical maps with a sufficient resolution and sensitivity to understand the sub-micron-scale distributions of potential by-product and deleterious elements. The technique is especially useful when the concentrations of those components are sufficiently low, as in the case of daughter radionuclides produced by uranium decay, which cannot be visualized by other techniques, such as LA-ICP-MS. NanoSIMS mapping is shown to be a valuable tool in determining the spatial distribution of trace elements and isotopes in fine-grained copper ores, providing researchers with

crucial evidence needed to answer questions of ore formation, and with major implications for the optimization of mineral processing.

In the final paper of this special issue, Cook et al. [34] use HAADF STEM imaging and STEM EDS mapping to address polysomatism and polytypism in modular, mixed-layer Pb-Bi-chalcogenide minerals belonging to the aleksite group. Focusing on a nanoscale characterization of unnamed $\text{PbBi}_4\text{Te}_4\text{S}_3$ in a specimen from Clogau, Wales (UK), the authors show that this phase occurs as at least three distinct polytypes within the same sample and go on to demonstrate how additional polysomes in the aleksite group can be derived by combinations of layers of different sizes. Atomic-scale STEM EDS mapping is used to confirm the sequence of individual atoms within individual layers of different sizes. This allows a revised definition of the group and prediction of additional structures, their chemistries, and stacking sequences.

3. Summary and Outlook

The reasoning behind the conference session and this special issue was to raise provocative topics that use nanoscale evidence to question existing models for ore-forming processes across the magmatic and hydrothermal spectrum. The idea that minerals are the best record of geochemical, geological, and ore-forming processes is certainly not new (e.g., the earlier special issue [35]), but the capabilities of present-day analytical techniques in terms of spatial resolution, sensitivity, and precision allow unparalleled insights into where, how, and when these processes happen. Although there are still unsolved problems with the preparation of samples for nanoscale studies (e.g., [16,36]), the papers in this issue represent examples of how an approach involving complementary analytical techniques can provide answers to petrological and mineralogical questions.

Changes in mineral signatures, phase associations, and zoning patterns are interpreted in terms of partitioning and cooling paths in magmatic systems [24,28]. The presence of critical metals, invisible gold in sulphides, and fluid–rock interactions in magmatic-hydrothermal systems are addressed for single deposits or ore provinces [23,25,27,29–32]. The mapping of trace elements in ore minerals using nanoSIMS is revolutionary in terms of its detection limits and spatial resolution, but also permits the visualization of transient radionuclides at ultra-trace concentrations [33]. Last but not least, the observation of multiple stacking sequences in mixed-layer compounds raises the issue of the identity of minerals [34].

The overall take home message we wish to convey is that minerals hold an untapped reservoir of information which will revolutionize our understanding of natural geochemical systems, if understood at appropriate scales of observations. At least one other forthcoming special issue of *Minerals* (Advances in Applying Electron Microscopy in Studying the Microstructure of Minerals; https://www.mdpi.com/journal/minerals/special_issues/TEM_Mineral) relates to the present one, as it also deals with the crystal structural modularity in minerals and its significance.

Author Contributions: C.L.C. and N.J.C. wrote this paper with contributions from the other Guest Editors: S.U., M.R., O.P.

Acknowledgments: The Guest Editors express their appreciation to Jingjing Yang and the *Minerals* editorial team for their encouragement and logistical assistance throughout this project. We also thank all reviewers for their time and comments. C.L.C. sincerely thanks Sumit Chakraborty for his initial encouragement to propose such a session for Goldschmidt 2018.

Conflicts of Interest: The authors declare no conflict of interest.

References

1. Hochella, M.F.J.; Lower, S.K.; Maurice, P.A.; Penn, R.L.; Sahai, N.; Sparks, D.L.; Twining, B.S. Nanominerals, Mineral Nanoparticles, and Earth Systems. *Science* **2008**, *319*, 1631–1635. [CrossRef]
2. Van Tendeloo, G.; Bals, S.; Van Aert, S.; Verbeeck, J.; Van Dyck, D. Advanced electron microscopy for advanced materials. *Adv. Mater.* **2012**, *24*, 5655–5675. [CrossRef]

3. Kilburn, M.R.; Wacey, D. Nanoscale secondary ion mass spectrometry (NanoSIMS) as an analytical tool in the geosciences. In *Principles and Practice of Analytical Techniques in Geosciences*; Royal Society of Chemistry: London, UK, 2015; pp. 1–34.
4. Valley, J.W.; Reinhard, D.A.; Cavosie, A.J.; Ushikubo, T.; Lawrence, D.F.; Larson, D.J.; Kelly, T.F.; Snoeyenbos, D.R.; Strickland, A. Nano- and micro-geochronology in Hadean and Archean zircons by atom-probe tomography and SIMS: New tools for old minerals. *Am. Mineral.* **2015**, *100*, 1355–1377. [[CrossRef](#)]
5. Cook, N.J.; Ciobanu, C.L.; George, L.; Zhu, Z.-Y.; Wade, B.; Ehrig, K. Trace Element Analysis of Minerals in Magmatic-Hydrothermal Ores by Laser Ablation Inductively-Coupled Plasma Mass Spectrometry: Approaches and Opportunities. *Minerals* **2016**, *6*, 111. [[CrossRef](#)]
6. Buddington, A.F.; Lindsley, D.H. Iron-titanium oxide minerals and synthetic equivalents. *J. Petrol.* **1964**, *5*, 310–357. [[CrossRef](#)]
7. Arguin, J.-P.; Pagé, P.; Barnes, S.-J.; Girard, R.; Duran, C. An integrated model for ilmenite, Al-spinel, and corundum exsolutions in titanomagnetite from oxide-rich layers of the Lac Doré Complex (Québec, Canada). *Minerals* **2018**, *8*, 476. [[CrossRef](#)]
8. Geisler, T.; Schaltegger, U.; Tomaschek, F. Re-equilibration of zircon in aqueous fluids and melts. *Elements* **2007**, *3*, 43–50. [[CrossRef](#)]
9. Ciobanu, C.L.; Cook, N.J.; Maunders, C.; Wade, B.P.; Ehrig, K. Focused ion beam and advanced electron microscopy for minerals: Insights and outlook from bismuth sulphosalts. *Minerals* **2016**, *6*, 112. [[CrossRef](#)]
10. Ciobanu, C.L.; Kontonikas-Charos, A.; Slattery, A.; Cook, N.J.; Ehrig, K.; Wade, B.P. Short-range stacking disorder in the bastnäsite-parisite compositional range: A HAADF-STEM study. *Minerals* **2017**, *7*, 227. [[CrossRef](#)]
11. Li, W.; Ciobanu, C.L.; Slattery, A.; Cook, N.J.; Liu, W.Y.; Wade, B.P.; Xie, G.Q. Chessboard structures: Atom-scale imaging of homologs from the kobellite series. *Am. Mineral.* **2019**, *104*, 459–462. [[CrossRef](#)]
12. Capitani, G. HRTEM investigation of bastnäsite–parisite intergrowths from Mount Malosa (Malawi): Ordered sequences, polysomatic faults, polytypic disorder, and a new parisite-(Ce) polymorph. *Eur. J. Mineral.* **2019**, *31*, 429–442. [[CrossRef](#)]
13. Dittrich, H.; Stadler, A.; Topa, D.; Schimper, H.-J.; Basch, A. Progress in sulfosalt research. *Phys. Stat. Sol.* **2009**, *206*, 1034–1041. [[CrossRef](#)]
14. Lee, M.R.; Bland, P.A.; Graham, G. Preparation of TEM samples by focused ion beam (FIB) techniques: Applications to the study of clays and phyllosilicates in meteorites. *Mineral. Mag.* **2003**, *67*, 581–592. [[CrossRef](#)]
15. Wirth, R. Focused Ion Beam (FIB) combined with SEM and TEM: Advanced analytical tools for studies of chemical composition, microstructure and crystal structure in geomaterials on a nanometre scale. *Chem. Geol.* **2009**, *261*, 217–229. [[CrossRef](#)]
16. Ciobanu, C.L.; Cook, N.J.; Utsunomiya, S.; Pring, A.; Green, L. Focussed ion beam–transmission electron microscopy applications in ore mineralogy: Bridging micro- and nanoscale observations. *Ore Geol. Rev.* **2011**, *42*, 6–31. [[CrossRef](#)]
17. Kusiak, M.A.; Dunkley, D.J.; Wirth, R.; Whitehouse, M.J.; Wilde, S.A.; Marquardt, K. Metallic lead nanospheres discovered in ancient zircons. *PNAS* **2015**, *112*, 4958–4963. [[CrossRef](#)]
18. Barra, F.; Deditius, A.; Reich, M.; Kilburn, M.R.; Guagliardo, P.; Roberts, M.P. Dissecting the Re-Os geochronometer. *Sci. Rep.* **2017**, *7*, 16054. [[CrossRef](#)]
19. Zhang, B.; Han, Z.X.; Wang, X.Q.; Liu, H.L.; Wu, H.; Feng, H. Metal-Bearing Nanoparticles Observed in Soils and Fault Gouges over the Shenjiayao Gold Deposit and Their Significance. *Minerals* **2019**, *9*, 414. [[CrossRef](#)]
20. Joshi, N.; Filip, J.; Coker, V.S.; Sadhukhan, J.; Safarik, I.; Bagshaw, H.; Lloyd, J.R. Microbial Reduction of Natural Fe(III) Minerals; Toward the Sustainable Production of Functional Magnetic Nanoparticles. *Front. Environ. Sci.* **2018**. [[CrossRef](#)]
21. Imoto, J.; Ochiai, A.; Furuki, G.; Suetake, M.; Ikehara, R.; Horie, K.; Takehara, M.; Yamasaki, S.; Nanba, K.; Ohnuki, T.; et al. Isotopic signature and nano-texture of cesium-rich micro-particles: Release of uranium and fission products from the Fukushima Daiichi Nuclear Power Plant. *Sci. Rep.* **2017**, *7*, 5409. [[CrossRef](#)]
22. Yin, S.; Wirth, R.; Ma, C.Q.; Xu, J.N. The role of mineral nanoparticles at a fluid-magnetite interface: Implications for trace-element uptake in hydrothermal systems. *Am. Mineral.* **2019**, *104*, 1180–1188. [[CrossRef](#)]

23. Crespo, J.; Reich, M.; Barra, F.; Verdugo, J.J.; Martínez, C. Critical Metal Particles in Copper Sulfides from the Supergiant Río Blanco Porphyry Cu–Mo Deposit, Chile. *Minerals* **2018**, *8*, 519. [[CrossRef](#)]
24. Baurier-Aymat, S.; Jiménez-Franco, A.; Roqué-Rosell, J.; González-Jiménez, J.M.; Gervilla, F.; Proenza, J.A.; Mendoza, J.; Nieto, F. Nanoscale structure of zoned laurites from the Ojén ultramafic massif, south Spain. *Minerals* **2019**, *9*, 288. [[CrossRef](#)]
25. Morishita, Y.; Hammond, N.Q.; Momii, K.; Konagaya, R.; Sano, Y.; Takahata, N.; Ueno, H. Invisible Gold in Pyrite from Epithermal, Banded-Iron-Formation-Hosted, and Sedimentary Gold Deposits: Evidence of Hydrothermal Influence. *Minerals* **2019**, *9*, 447. [[CrossRef](#)]
26. Reich, M.; Kesler, S.E.; Utsunomiya, S.; Palenik, C.S.; Chryssoulis, S.L.; Ewing, R.C. Solubility of gold in arsenian pyrite. *Geochim. Cosmochim. Acta* **2005**, *69*, 2781–2796. [[CrossRef](#)]
27. Xu, J.; Ciobanu, C.L.; Cook, N.J.; Slattery, A. Crystals from the Powellite-Scheelite Series at the Nanoscale: A Case Study from the Zhibula Cu Skarn, Gangdese Belt, Tibet. *Minerals* **2019**, *9*, 340. [[CrossRef](#)]
28. Gao, W.; Ciobanu, C.L.; Cook, N.J.; Slattery, A.; Huang, F.; Song, D. Nanoscale study of titanomagnetite from the Panzhihua layered intrusion, Southwest China: Multistage exsolutions record ore formation. *Minerals* **2019**, *9*, 513. [[CrossRef](#)]
29. Keyser, W.; Ciobanu, C.L.; Cook, N.J.; Feltus, H.; Johnson, G.; Slattery, A.; Wade, B.P.; Ehrig, K. Mineralogy of zirconium in iron-oxides: A micron- to nanoscale study of hematite ore from Peculiar Knob, South Australia. *Minerals* **2019**, *9*, 244. [[CrossRef](#)]
30. Ciobanu, C.L.; Verdugo-Ihl, M.R.; Slattery, A.; Cook, N.J.; Ehrig, K.; Courtney-Davies, L.; Wade, B.P. Silician magnetite: Si-Fe-nanoprecipitates and other mineral inclusions in magnetite from the Olympic Dam deposit, South Australia. *Minerals* **2019**, *9*, 311. [[CrossRef](#)]
31. Verdugo-Ihl, M.R.; Ciobanu, C.L.; Slattery, A.; Cook, N.J.; Ehrig, K.; Courtney-Davies, L. Copper-arsenic nanoparticles in hematite: Fingerprinting fluid-mineral interaction. *Minerals* **2019**, *9*, 388. [[CrossRef](#)]
32. Courtney-Davies, L.; Ciobanu, C.L.; Verdugo-Ihl, M.R.; Slattery, A.; Cook, N.J.; Dmitrijeva, M.; Keyser, W.; Wade, B.P.; Domnick, U.I.; Ehrig, K.; et al. Zircon at the nanoscale records metasomatic processes leading to large magmatic-hydrothermal ore systems. *Minerals* **2019**, *9*, 364. [[CrossRef](#)]
33. Rollog, M.; Cook, N.J.; Guagliardo, P.; Ehrig, K.J.; Ciobanu, C.L.; Kilburn, M. Detection of trace elements/isotopes in Olympic Dam copper concentrates by nanoSIMS. *Minerals* **2019**, *9*, 336. [[CrossRef](#)]
34. Cook, N.J.; Ciobanu, C.L.; Liu, W.Y.; Slattery, A.; Mills, Stanley, C.J. Polytypism and polysomatism in mixed-layer chalcogenides: Characterization of $\text{PbBi}_4\text{Te}_4\text{S}_3$ and inferences for ordered phases in the aleksite series. *Minerals* **2019**, *9*, 628. [[CrossRef](#)]
35. Reich, M.; Hough, R.; Deditius, A.; Utsunomiya, S.; Ciobanu, C.; Cook, N. (Eds.) *Nanogeoscience in Ore Systems Research: Principles, Methods, and Applications*; Special Issue of Ore Geology Reviews; Elsevier: Amsterdam, The Netherlands, 2011; Volume 42, pp. 1–84.
36. Capitani, G. Bizarre artefacts in transmission electron microscopy preparation and observation of geological samples. *Eur. J. Mineral.* **2019**, in press.



© 2019 by the authors. Licensee MDPI, Basel, Switzerland. This article is an open access article distributed under the terms and conditions of the Creative Commons Attribution (CC BY) license (<http://creativecommons.org/licenses/by/4.0/>).